INTERNATIONAL JOURNAL OF PHARMACEUTICAL RESEARCH AND BIOMEDICAL ANALYSIS | ISSN: 2278 –2664
| APR-JUN 2025 | VOLUME 14 | ISSUE 2 | 85-105
Available Online Through: www.ijprba.com

Research Article

DEVELOPMENT AND OPTIMIZATION OF SOLID LIPID NANOPARTICLES OF DASATINIB USING DESIGN OF EXPERIMENTS: *IN VITRO* DRUGRELEASE AND *IN-VIVO* PHARMACOKINETIC STUDIES

Chandu Vamshi Gangula[1*], Seema Tomar[2], and [3]Poli Reddy Papagatla

[*]Research Scholar, Faculty of Pharmaceutical Sciences, Motherhood University, Dehradun Road, Karoundi Village, Bhagwanpur post, Roorkee Tehsil, Haridwar Distt., Uttarakhand, India 247661.

[1]Professor, Faculty of Pharmaceutical Sciences, Motherhood University, Dehradun Road, Karoundi Village, Bhagwanpur post, Roorkee Tehsil, Haridwar Distt., Uttarakhand, India 247661.

[2]Professor, Nalanda College Of Pharmacy, Nalgonda, Telangana, India.

Email: gcvyadav@gmail.com

ABSTRACT

Dasatinib, a potent BCR-ABL tyrosine kinase inhibitor, suffers from poor aqueous solubility and pH-dependent absorption, leading to variable bioavailability and frequent dosing in leukemia therapy. Solid lipid nanoparticles (SLNs) offer a promising strategy to enhance solubility, prolong release, and improve systemic exposure. This study developed and optimized Dasatinib-loaded SLNs using a Box-Behnken design to systematically evaluate the effects of lipid weight (500–1000 mg), surfactant concentration (0.5–2% w/v), and homogenization time (4–10 min) on critical quality attributes. The optimized SLNs (900 mg lipid, 1.75% surfactant, 8.5 min homogenization) exhibited a particle size of 204 nm, zeta potential of -27.3 mV, and entrapment efficiency of 85.8%, closely matching predicted values (R^2 > 0.94). FTIR and DSC confirmed successful drug encapsulation within the lipid matrix, while SEM revealed spherical, monodisperse nanoparticles. In vitro release studies demonstrated sustained drug release (95% at 24 h) following the Korsmeyer-Peppas model (R^2 = 0.995, n = 0.56), indicating combined diffusion-erosion mechanisms. In vivo pharmacokinetics in rats showed a 1.6-fold increase in AUC and prolonged Tmax (8 h vs. 2 h for pure drug), confirming enhanced bioavailability. These results highlight the potential of SLNs to overcome Dasatinib's delivery challenges, offering a scalable nanocarrier system for improved leukemia treatment.

KEY WORDS

Dasatinib, Nanoparticles, Stearic acid, Design of experiments, In vivo pharmacokinetics.

1. INTRODUCTION

Dasatinib is a potent, orally active, second-generation tyrosine kinase inhibitor (TKI) that has gained regulatory approval for the treatment of chronic myeloid leukemia (CML) and Philadelphia chromosome-positive acute lymphoblastic leukemia (Ph+ ALL) [1,2]. It functions by inhibiting a wide spectrum of tyrosine kinases, including BCR-ABL, SRC family kinases, c-KIT, PDGFR, and ephrin receptors [3]. Its enhanced efficacy against imatinib-resistant BCR-ABL mutations has positioned it as a valuable agent in frontline as well as second-line therapy for patients with resistant or intolerant

forms of leukemia [4,5]. However, despite its therapeutic benefits, Dasatinib is associated with several pharmacokinetic and biopharmaceutical limitations that significantly restrict its clinical performance and oral bioavailability.

According to the Biopharmaceutical Classification System (BCS), Dasatinib falls under Class II, characterized by high permeability but low aqueous solubility [6, 7]. Its solubility in water is exceedingly poor (approximately 0.008 mg/mL at 25 °C), and its dissolution behavior is strongly pH-dependent, with high solubility observed in acidic conditions (pH < 3) and rapid decline in solubility at neutral and basic pH [8, 9]. This presents a considerable challenge for consistent oral absorption, especially in the gastrointestinal environment, where pH can vary significantly along the GI tract and is influenced by the presence of food or co-administered medications (e.g., antacids, H_2-blockers, or proton pump inhibitors). Additionally, Dasatinib undergoes extensive first-pass metabolism primarily through the cytochrome P450 enzyme CYP3A4, further reducing its systemic availability and leading to a relatively short half-life (~3–5 hours), necessitating frequent dosing to maintain therapeutic plasma levels [10, 11]. Collectively, these challenges highlight the urgent need for advanced formulation strategies to enhance the solubility, stability, and oral bioavailability of Dasatinib.

Over the past decade, lipid-based nanocarriers, particularly Solid Lipid Nanoparticles (SLNs), have emerged as a promising platform for the delivery of poorly water-soluble drugs [12-14]. SLNs are submicron colloidal systems composed of biodegradable and biocompatible solid lipids dispersed in an aqueous surfactant solution. They offer several formulation-related and pharmacokinetic advantages, including improved solubilization of lipophilic drugs, enhanced protection against hydrolytic and oxidative degradation, controlled and sustained drug release, improved lymphatic absorption, and bypassing of first-pass hepatic metabolism, which can substantially enhance systemic bioavailability [15-17]. Moreover, SLNs are relatively simple to manufacture, scalable, and have shown excellent safety profiles in both preclinical and clinical settings. The solid matrix of SLNs can encapsulate lipophilic drugs like Dasatinib efficiently, while the surfactant layer helps maintain colloidal stability, minimize aggregation, and facilitate transport across biological membranes.

The present study was therefore undertaken with the aim of formulating and optimizing Dasatinib-loaded Solid Lipid Nanoparticles (Dasatinib-SLNs) using the hot homogenization followed by ultrasonication method, a widely adopted and scalable approach for SLN fabrication. To systematically investigate the influence of critical formulation and process variables, a Box–Behnken Design (BBD) was employed. Three independent variables lipid weight, surfactant concentration, and homogenization time were selected based on preliminary trials and literature evidence. These variables were evaluated for their effects on key dependent responses, namely particle size, zeta potential, and entrapment efficiency, which are critical determinants of nanoparticle performance, stability, and in vivo fate. The application of design of experiments (DoE) enabled the generation of predictive models, identification of significant factor interactions, and determination of an optimized formulation using Derringer's desirability function.

Following optimization, the Dasatinib-SLNs were characterized for physicochemical parameters including particle morphology and in vitro drug release profile. This study aims to establish a

robust and reproducible SLN-based delivery system that can overcome the solubility and bioavailability challenges of Dasatinib, thereby improving its therapeutic index and patient compliance in the treatment of hematologic malignancies.

2. MATERIALS AND METHODS

2.1. Materials

Dasatinib HCl was kind gift sample from RX Innovation Pvt Ltd, Hyderabad, India. Stearic acid and Poloxamer 188 were procured from Sd Fine Chem Ltd, Hyderabad, India.

2.2. Design of Experiments

A Box–Behnken Design (BBD) was employed to optimize the formulation of Dasatinib-loaded solid lipid nanoparticles (SLNs) and to evaluate the influence of key formulation and process variables on selected critical quality attributes. The experimental design was generated using Design-Expert® software (version XX, Stat-Ease Inc., Minneapolis, USA). Three independent variables were selected: lipid weight (X_1, 50–100 mg), surfactant concentration (X_2, 0.5–2% w/v), and homogenization time (X_3, 4–10 minutes) (Table 1). Each factor was studied at three levels (low, medium, and high), and the BBD included a total of 17 experimental runs, including five center points to estimate experimental error [18, 19].

Table 1: Independent Variables and Measured Responses for Box–Behnken Design Used in the Optimization of Dasatinib-Loaded SLNs

Type	Variable	Code	Level Range	Unit
Independent Factors	Lipid weight	X_1	50 – 100	mg
	Surfactant concentration	X_2	0.5 – 2.0	% w/v
	Homogenization time	X_3	4 – 10	minutes
Dependent Responses	Particle size	Y_1	Minimize	nm
	Zeta potential	Y_2	Minimize	mV
	Entrapment efficiency	Y_3	Maximize	%

The dependent variables (responses) considered for optimization were particle size (Y_1), zeta potential (Y_2), and entrapment efficiency (Y_3). The primary goal of the optimization was to minimize particle size, maximize entrapment efficiency, and zeta potential values to ensure physical stability of the SLN dispersion. All formulations were prepared using the hot homogenization followed by ultrasonication technique described in section 2.2. The experimental data obtained were fitted to a second-order quadratic polynomial model, and analysis of variance (ANOVA) was used to evaluate the significance of individual variables and their interactions. The adequacy of the model was assessed based on statistical parameters such as the coefficient of determination (R^2), adjusted R^2, and the lack-of-fit test. Three-dimensional response surface plots were generated to visualize the interactions among formulation variables and their effects on the responses. The optimized formulation was selected using Derringer's desirability function, and the model was validated by comparing the predicted values with the experimental results for the optimized batch.

2.3. Preparation of Dasatinib-Loaded Solid Lipid Nanoparticles (SLNs)

Dasatinib-loaded solid lipid nanoparticles were prepared using a hot homogenization followed by ultrasonication technique, incorporating a three-factor optimization approach based on lipid weight, surfactant concentration, and homogenization time. Briefly, the required amount of stearic acid (solid lipid) was accurately weighed and melted at 70–75 °C in a thermostatically controlled water bath. Dasatinib (100 mg) was dispersed into the molten lipid with continuous magnetic stirring to ensure uniform drug distribution. In parallel, the aqueous phase was prepared by dissolving Poloxamer 188 (selected surfactant) at the desired concentration in distilled water, which was also preheated to the same temperature to prevent premature solidification of the lipid.

The hot lipid phase was then gradually added to the aqueous phase under high-speed homogenization (IKA Ultra-Turrax T25) at 10,000–15,000 rpm for a predetermined duration based on the experimental design. The resulting hot coarse emulsion was subsequently subjected to probe ultrasonication (QSonica Q700, 20 kHz) in pulse mode (5 seconds ON, 5 seconds OFF) for 5 minutes in an ice bath to reduce particle size and improve dispersion uniformity. The nano emulsion was then allowed to cool to room temperature under gentle stirring, leading to the formation of SLNs as the lipid recrystallized. For lyophilized formulations, mannitol (5% w/v) was added as a cryoprotectant prior to freeze-drying using a laboratory lyophilizer (Labconco FreeZone, USA) at −40 °C for 48 hours. All formulations were prepared in triplicate and stored at 4 °C in airtight containers until further characterization [20].

2.4. Characterization of Dasatinib-SLNs [20]

2.4.1. Particle size and *polydispersity index (PDI) and analysis*

The particle size of all produced Dasatinib-SLNs batches was assessed using equipment from Malvern Instruments Ltd, Worcestershire, UK. This analysis aimed to determine the uniformity of particle size distribution and the size range of the Dasatinib-SLNs. Prior to each analysis, the Dasatinib-SLNs were suitably diluted with distilled water [17].

2.4.2. Zeta Potential

Zeta potential measurement serves to assess the surface charge of the particles and was conducted to evaluate the stability of the nanoparticles within the suspension. The zeta potential (ZP) of these developed formulations was measured using a Zetasizer, from Malvern Instruments Ltd, Worcestershire, UK. The instrument was operated at a constant room temperature, employing a clean, disposable zeta cell [17]. The average particle size, polydispersity index (PDI), and zeta potential (ZP) of the Dasatinib-SLNs were determined and then averaged from three independent measurements.

2.4.3. Entrapment Efficiency and Drug loading

For encapsulation studies, the dispersion of Dasatinib-SLNs was centrifuged at 20,000 rpm at 4^0C for 30 min using a cold centrifuge (Sigma Labort Centrifuge GmbH, Germany). After centrifugation, the supernatant and the precipitation obtained were separated and analysed for the drug concentration using a UV spectrophotometer at wavelength 236nm [17].

The encapsulation efficiency and percent drug loading were calculated using the following formulae:

$$\%Encapsulation\ Efficiency = \frac{Amount\ of\ drug\ encapsulated}{Drug\ amount\ added\ initially\ in\ the\ formula} \times 100$$

$$\%Drug\ Loading = \frac{Amount\ of\ drug\ encapsulated}{Weight\ of\ Nanoparticles} \times 100$$

2.4.4. FTIR Studies

FTIR spectra were generated for various substances, including pure Dasatinib, Lauric acid, polysorbate 80, and the optimized Dasatinib-SLNs. This was accomplished by blending these samples with FTIR-grade KBr and compressing the mixture into transparent pellets using a die. The scanning process covered a wavenumber range from 4000 to 400 cm^{-1} with Bruker Tensor FTIR instrument. In this analysis, each sample was exposed to infrared (IR) photons, allowing for the identification of distinctive functional group signatures within the chemical compounds. These spectral fingerprints were utilized to infer potential chemical interactions occurring between the drug, formulation ingredients and also nanoparticles [17].

2.4.5. Thermal Analysis by Differential Scanning calorimetry

DSC (Differential Scanning Calorimetry) curves were generated for pure Dasatinib, Stearic acid, and the optimized Dasatinib-SLNs using a thermos-analytical technique employing the Scinco N650 instruments, Korea. Each sample of 5 mg quantity, was tightly packed into a hemispherical aluminium pan, individually placed adjacent to a reference pan left empty. The analysis chamber was supplied with nitrogen at a flow rate of 20 mL/min, and the temperature was incrementally increased at a rate of 20 °C within the range of 50–300 °C[17].

2.4.6. Surface Morphology

The surface morphology of the optimized Dasatinib-SLNs was assessed through Scanning Electron Microscopy (SEM) using a Zeiss EVO LS10 instrument. The sample was affixed onto a stub and subjected to a gold-sputter process for coating before imaging was conducted [17].

2.4.7. *Invitro* Drug release study and Kinetic modelling

In-vitro drug release studies of pure Dasatinib and optimized Dasatinib-SLNs were conducted using dialysis bag (Hi-media Mol. 12,000 Dalton) diffusion technique. The sample of Dasatinib-SLNs (Weight equivalent to 150mg of Dasatinib) was sealed in the dialysis membrane bag.The dialysis bag was placed in the cylindrical vessel of a USP Dissolution Apparatus II (Lab India DS 8000, Mumbai, India) containing 200 mL of dissolution medium (0.1N HCl), maintained at 37 ± 0.5 °C, with a rotation speed set to 75 rpm. At pre-determined time interval (0.5, 1, 2, 4, 6, 8, 12, and 24h) 2 mL sample is withdrawn from outer solution at each time interval and replaced by fresh 0.1N HCl medium to maintain sink conditions. The aliquots were filtered and analysed for drug release by using UV-spectrophotometer at 236nm (Jasco V-630 Made in Japan). The experiment was done in triplicate. The drug release data underwent fitting to various kinetic models, including the zero-order, first-order, Higuchi, and Korsmeyer-Peppas models. These models were applied by establishing relationships between the percentage of drug release per unit time, the percentage of log cumulative drug release per unit time, the percentage of log cumulative drug release per unit square root of time, and the percentage of log cumulative drug release per unit log of time, respectively. The selection of the

most appropriate model for describing the medication release was determined based on the highest correlation coefficient value (R^2). Additionally, the release-exponent, which provides insights into the mechanism of drug release, was calculated using the slope and R^2 values obtained from the respective plots [17].

2.4.8. *In-vivo* Pharmacokinetics Study

Female Sprague Dawley rats (180–200 g) were procured from the animal facility of Ziva Life Sciences. The study was conducted following approval from the Institutional Animal Ethics Committee (IAEC), Jeeva Life Sciences, Hyderabad, India (1757/PO/RcBiBtNRc/S/14/CPCSEA). Animals were housed under controlled conditions (25 ± 2°C, 50–60% relative humidity) with natural light/dark cycles and acclimatized for one week prior to the experiment. The rats were randomly assigned to two groups (n = 5 per group). Following an overnight fast (12 h) with ad libitum access to water, Group 1 received Dasatinib orally at a dose equivalent to 10 mg/kg of Dasatinib, while Group 2 received Dasatinib suspended in 0.2% w/v carboxymethyl cellulose at the same dose. Blood samples (250 µL) were collected from the tail vein into heparinized microcentrifuge tubes at predetermined time intervals (0.5, 1, 2, 4, 6, 8, 12, and 24 h). The samples were centrifuged at 10,000 rpm for 5 minutes to separate plasma, which was then stored at –20°C until analysis [18]. Plasma concentrations of dasatinib were quantified using a previously validated HPLC method [19]. The non-compartmental pharmacokinetic evaluation was carried out using the "Phoenix WinNonlin PK/PD Analysis Tool" developed by Certara, USA, in order to determine a range of pharmacokinetic parameters. The results were expressed as mean ± standard deviation (SD). Pharmacokinetic parameters, including peak plasma concentration (C_{max}), time to reach peak concentration (T_{max}), area under the curve (AUC), and [(AUC_{0-24}) ($AUC_{0-\infty}$)], half-life ($T_{1/2}$), rate constant (Kz), mean residence time (MRT), were estimated. An unpaired t-test was used to statistically compare the Dasatinib-SLNs formulation and the standard Dasatinib suspension. The level of statistical significance was chosen at $p < 0.05$.

3. RESULTS AND DISCUSSION

3.1. Experimental design

A Box-Behnken design was employed to evaluate the influence of three independent variables—lipid weight (500–1000 mg), surfactant concentration (0.5–2% w/v), and homogenization time (4–10 min) on critical quality attributes of Dasatinib-loaded solid lipid nanoparticles (SLNs), namely particle size, zeta potential, and entrapment efficiency (EE%).

The summary of the experimental design results was enumerated in Table 2. The effect of independent factor on the response variables were discussed below.

Table 2: Box–Behnken Design Matrix for Dasatinib-SLNs: Formulation Variables and Responses

Run	Factor 1	Factor 2	Factor 3	Response 1	Response 2	Response 3
	A: Lipid Weight	B: Surfactant Concentration	C: Homogenization time	Particle Size	Zeta Potential	Entrapment Efficiency
	mg	%w/v	min	nm	mV	%
1	750	2	4	280	71.3	-18.6
2	500	1.25	10	295	59.2	-15.01
3	750	0.5	10	281	69.2	-15.6
4	1000	1.25	4	256	79.8	-19.87
5	500	0.5	7	330	52.7	-14.3
6	750	1.25	7	223	83.4	-21.6
7	1000	2	7	235	80.5	-27.8
8	750	1.25	7	214	86.9	-22.8
9	750	0.5	4	259	71.5	-18.5
10	1000	0.5	7	261	72.3	-19.4
11	750	1.25	7	207	81.5	-21.5
12	750	1.25	7	219	82.2	-22.5
13	500	2	7	329	64.9	-15.1
14	750	2	10	225	82.5	-24.7
15	500	1.25	4	345	55.9	-14.06
16	1000	1.25	10	221	81.6	-27.07
17	750	1.25	7	203	84.8	-23.2

3.1.1. Particle Size Analysis of Dasatinib-SLNs

The influence of critical formulation parameters lipid weight (A), surfactant concentration (B), and homogenization time (C) on the particle size of Dasatinib-loaded solid lipid nanoparticles (SLNs) was assessed using a Box-Behnken design. Model fit statistics indicated that a quadratic model best described the experimental data, as evidenced by a high adjusted R^2 (0.9578) and predicted R^2 (0.8219), with a non-significant lack-of-fit ($p = 0.3054$), supporting the model's robustness and predictive capacity.

Analysis of variance (ANOVA) revealed the model's statistical significance ($p < 0.0001$; $F = 41.31$). Among the factors, lipid weight exerted the most profound effect ($p < 0.0001$), followed by homogenization time ($p = 0.0030$), while surfactant concentration showed a borderline significance ($p = 0.0525$). An increase in lipid concentration led to larger particle sizes, likely due to the formation of larger lipid droplets, whereas prolonged homogenization time reduced particle size due to enhanced shear-mediated droplet breakdown.

The interaction between surfactant concentration and homogenization time (BC) was significant ($p = 0.0046$), indicating a synergistic influence on nanoparticle size reduction. However, the AB and AC interactions were not significant, suggesting limited

combined effects. Quadratic terms A^2, B^2, and C^2 were all highly significant ($p < 0.01$), confirming non-linear relationships and further validating the model choice.

The regression equation derived for particle size was:

Particle Size (nm) = 213.2 – 40.75A – 7.75B – 14.75C – 6.25AB + 3.75AC – 19.25BC + 46.78A^2 + 28.78B^2 + 19.28C^2

Graphical illustrations such as the perturbation plot (Figure 1a) identified lipid weight as the most critical variable, while the contour (Figure 1b) and 3D response surface plots (Figure 1c) visually delineated the optimal regions for achieving minimal particle size.

3.1.2. Zeta Potential of Dasatinib-SLNs

The surface charge behavior of Dasatinib-loaded SLNs, expressed as zeta potential, was also evaluated using the same design. The quadratic model provided the best fit, with an adjusted R^2 of 0.9600 and a predicted R^2 of 0.8265, supported by a non-significant lack-of-fit ($p = 0.2813$).

The ANOVA indicated strong statistical significance ($p < 0.0001$; $F = 43.69$). Lipid weight was the most influential factor ($p < 0.0001$; $F = 210.40$), showing an inverse relationship with zeta potential, likely due to decreased surface charge density with higher lipid content. Surfactant concentration ($p = 0.0001$) and homogenization time ($p = 0.0024$) also significantly affected zeta potential, likely by modulating the surface coverage and uniformity of nanoparticles.

Notably, interactions between factors—AB ($p = 0.0033$), AC ($p = 0.0088$), and BC ($p = 0.0013$)—were all significant, indicating complex interdependencies influencing surface charge. All three quadratic terms were also significant, supporting the model's non-linear nature.

The resulting polynomial equation was:

Zeta Potential (mV) = 22.32 – 4.45875A – 2.3B – 1.41875C – 1.9AB – 1.5625AC – 2.25BC + 1.75875A^2 + 1.41125B^2 + 1.55875C^2

The perturbation plot (Figure 2a) confirmed lipid weight as the primary influencer of zeta potential, while Figures 2b and 2c (contour and 3D plots, respectively) showed optimal zeta potential values occurring within balanced formulations, suggesting improved nanoparticle stability under these conditions.

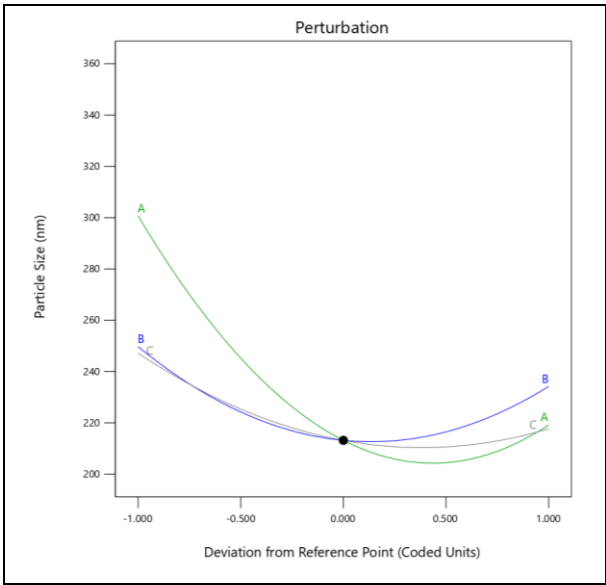

1a

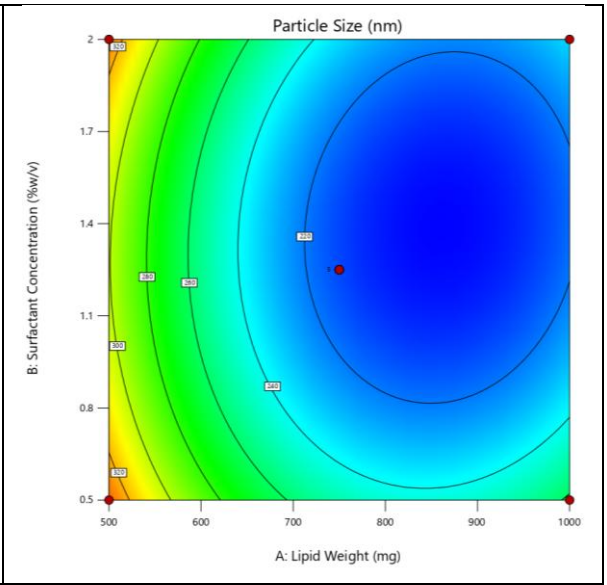

1b

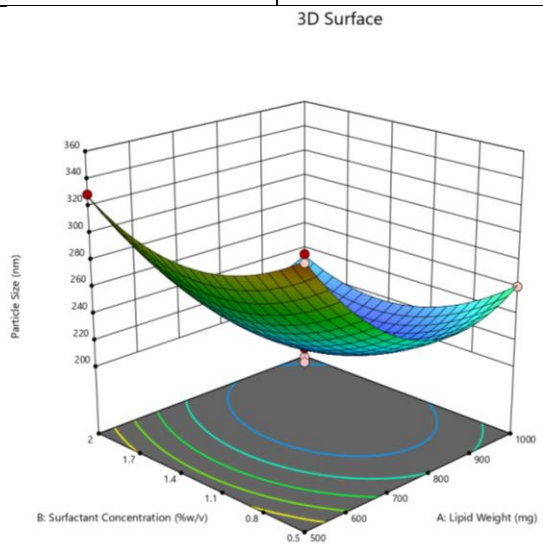

1c

Figure 1: (a) Perturbation plot showing the influence of lipid weight (A), surfactant concentration (B), and homogenization time (C) on particle size. **(b)** Contour plot illustrating the interactive effect of lipid weight and surfactant concentration on particle size at a fixed homogenization time. **(c)** 3D response surface plot showing the effect of lipid weight and homogenization time on particle size, confirming non-linear behaviour.

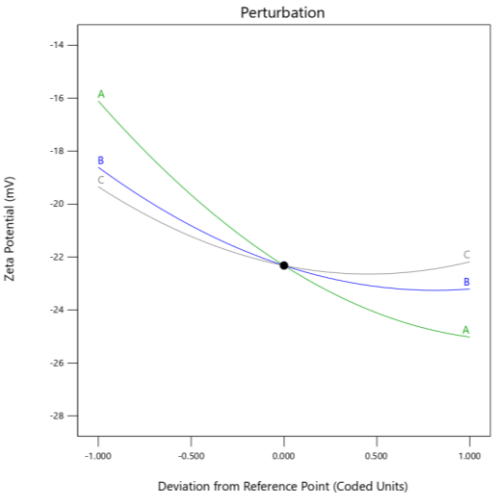

2a

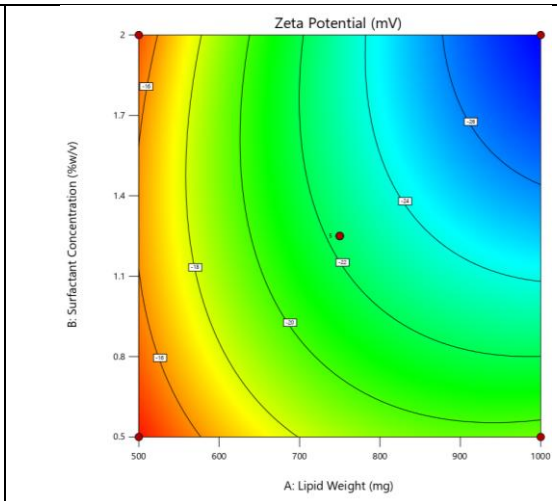

2b

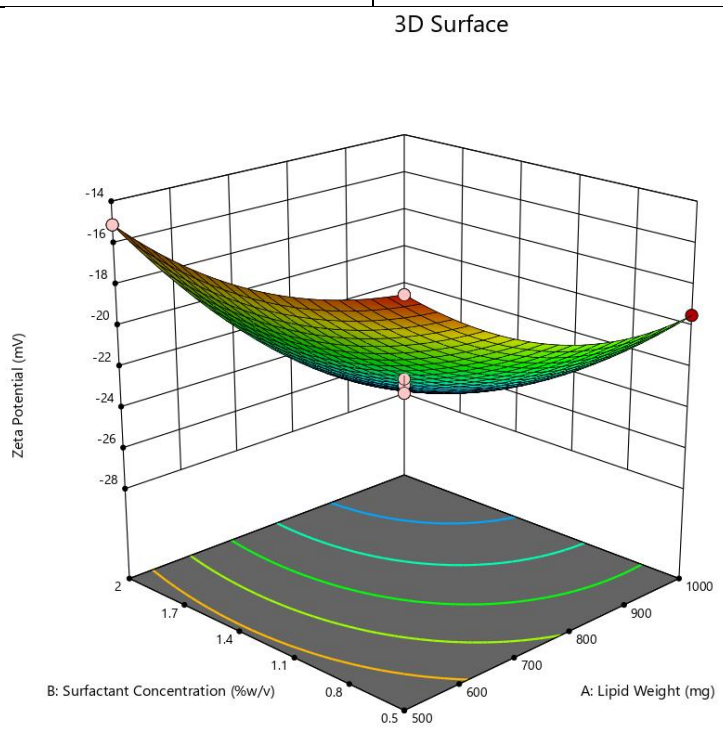

2c

Figure 2: (a) Perturbation plot depicting the effect of individual formulation factors on zeta potential. **(b)** Contour plot showing the interactive influence of lipid weight and surfactant concentration on zeta potential. **(c)** 3D response surface plot demonstrating how lipid weight and homogenization time modulate zeta potential.

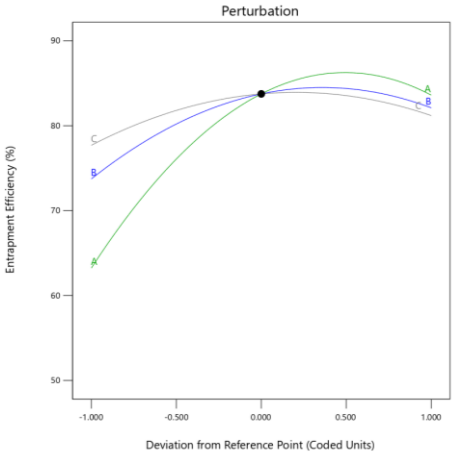

3a

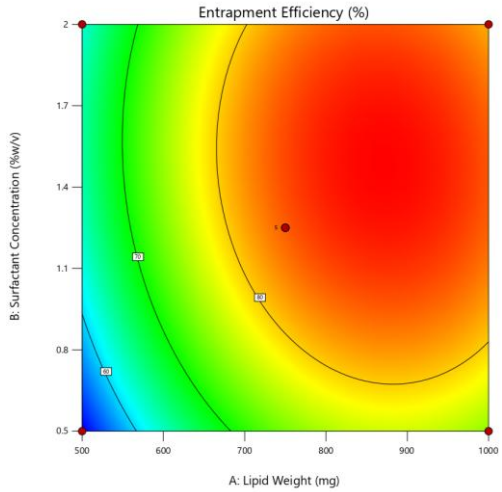

3b

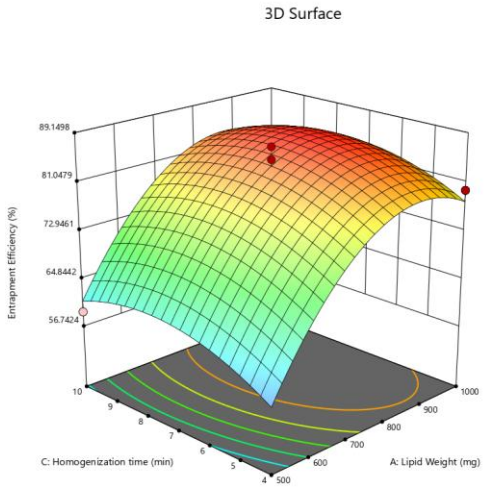

3c

Figure 3: (a) Perturbation plot showing the relative impact of lipid weight, surfactant concentration, and homogenization time on EE%. **(b)** Contour plot displaying the interaction between lipid weight and surfactant concentration on EE%. **(c)** 3D response surface plot illustrating the combined effect of surfactant concentration and homogenization time on EE%.

3.1.3. Entrapment Efficiency of Dasatinib-SLNs

Entrapment efficiency (EE%) was significantly impacted by formulation variables as per the Box-Behnken design. The quadratic model demonstrated an excellent fit (adjusted R^2 = 0.9467; predicted R^2 = 0.7746) with a non-significant lack-of-fit (p = 0.3021), indicating high model reliability.

ANOVA confirmed model significance ($p < 0.0001$; F = 32.60), with lipid weight being the most impactful factor ($p < 0.0001$), followed by surfactant concentration (p = 0.0019). Homogenization time showed moderate influence (p = 0.0845). The BC interaction term

was significant ($p = 0.0289$), suggesting improved EE% when surfactant concentration and homogenization time are tuned together. Other interactions (AB, AC) were not significant. Quadratic terms for all three variables ($p < 0.01$) supported the existence of curvature in the response surface.

The regression equation was:

Entrapment Efficiency (%) = $83.76 + 10.19A + 4.19B + 1.75C - 1AB - 0.375AC + 3.375BC - 10.33A^2 - 5.83B^2 - 4.31C^2$

Perturbation analysis (Figure 3a) showed lipid weight as the major determinant of EE%, supported by contour (Figure 3b) and 3D surface plots (Figure 3c), which revealed high entrapment values at intermediate to high lipid and surfactant levels.

The Box-Behnken experimental design effectively optimized key formulation parameters for Dasatinib-loaded SLNs. Lipid weight emerged as the dominant factor influencing all three responses—particle size, zeta potential, and entrapment efficiency. Surfactant concentration and homogenization time also played important roles, either directly or via interactive effects. All responses showed non-linear behavior, justifying the use of a quadratic model. The statistical analysis, regression modeling, and graphical interpretation collectively facilitated the identification of optimal formulation conditions that yield SLNs with desirable physicochemical properties for improved drug delivery.

EXPERIMENTAL OPTIMIZATION

Optimization and Validation of Dasatinib-Loaded Solid Lipid Nanoparticles

Numerical optimization was employed to develop an optimal dasatinib-loaded SLN formulation, with the goal of minimizing particle size and zeta potential while maximizing entrapment efficiency (EE). The optimized formulation comprised 900mg lipid, 1.75% surfactant, and 8.5mins homogenization time, yielding predicted values of 202.3 nm particle size, -27.7 mV zeta potential, and 86.7% EE. Experimental validation confirmed the model's reliability, with observed values of 204 nm (1.7 nm deviation), -27.3 mV (1.6% variation), and 85.8% EE (1.0% below prediction). The close agreement between predicted and experimental results underscores the robustness of the optimization approach. The MODR overlay plot (Figure 4) further verified that all responses fell within the acceptable design space, ensuring compliance with nanotechnology standards for drug delivery.

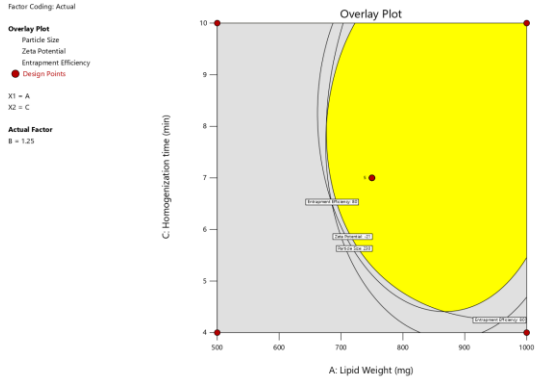

Figure 4: MODR Overlay Plot Demonstrating the Design Space for Optimized Dasatinib-Loaded SLNs

3.2. Characterization of Dasatinib-SLNs

The particle size ranged from 203 to 345 nm, with the smallest size observed at the midpoint levels of all factors (750 mg lipid, 1.25% surfactant, 7 min homogenization). Zeta potential values ranged between –14.06 and –27.8 mV, indicating moderate to good stability of the formulations. Entrapment efficiency varied significantly from 52.7% to 86.9%, with the highest EE observed at optimized conditions (750 mg lipid, 1.25% surfactant, and 7 min homogenization), highlighting the strong influence of factor interactions on drug loading capacity.

3.2.1. FTIR Analysis

The FTIR spectra of pure dasatinib, stearic acid, and dasatinib-loaded SLNs were recorded (Figure 5) to evaluate potential interactions between the drug and the lipid matrix, as well as to confirm successful incorporation of dasatinib into the SLNs.

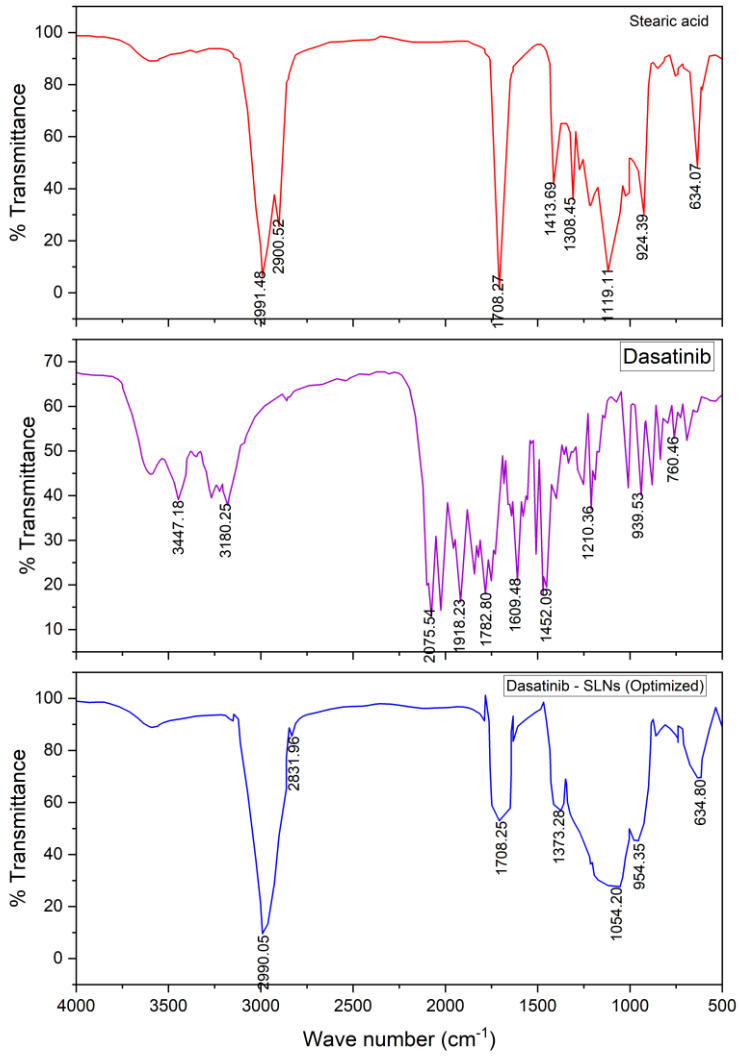

Figure 5: FTIR spectra of Dasatinib, stearic acid and Dsastinib-SLNs

Dasatinib exhibited characteristic peaks at 3447.18 cm^{-1} and 3180.25 cm^{-1} corresponding to N–H and O–H stretching vibrations, indicative of the presence of secondary amine or hydrogen-bonded functionalities. A strong absorption at 1782.80 cm^{-1} corresponds to the C=O stretching vibration from the amide or thiazole carboxamide moiety, which is a key structural feature of dasatinib. The aromatic C=C stretching vibration appeared at 1609.48 cm^{-1}, while additional peaks at 1210.36 and 939.53 cm^{-1} were assigned to C–N (aromatic amine) and C–Cl stretches, respectively, consistent with the presence of chlorophenyl and aromatic amine groups in the drug molecule.

In the FTIR spectrum of stearic acid, the major peaks include asymmetric and symmetric C–H stretching vibrations at 2991.48 and 2900.52 cm^{-1}, respectively, confirming the presence of long alkyl chains. A sharp peak at 1708.27 cm^{-1} is attributed to the C=O stretching of the carboxylic acid dimer, which is a hallmark of solid-state fatty acids. Additional vibrations at 1413.69 cm^{-1} (CH_2 scissoring or O–H bending), 1308.45 cm^{-1} (C–O and O–H bending), and 1119.11 cm^{-1} (C–O stretch) further confirm the presence of the carboxylic acid group and its dimeric hydrogen bonding network.

Upon analysis of the Dasatinib-loaded SLNs, several spectral changes were observed, suggesting interactions between dasatinib and the lipid matrix. The C–H asymmetric and symmetric stretches appeared at 2990.05 and 2831.96 cm^{-1}, respectively, both shifted slightly from their original positions in pure stearic acid. These shifts indicate conformational changes in the lipid alkyl chains, possibly due to dasatinib intercalation. The C=O stretch at 1708.25 cm^{-1} remained nearly unchanged, reflecting the retention of the stearic acid's carboxylic acid dimer; however, the slight shift may suggest weak hydrogen bonding between the drug's carbonyl groups and the lipid matrix.

A notable peak at 1054.20 cm^{-1}, assigned to C–O or ester-type vibrations, could arise from surfactant (e.g., Poloxamer 188) or new interactions between dasatinib and the lipid environment. Additionally, the O–H out-of-plane bending at 954.35 cm^{-1}, shifted from 924.39 cm^{-1} (pure stearic acid), indicates partial disruption of the native hydrogen bonding network within stearic acid, likely due to drug incorporation. The C–C skeletal vibration at 634.80 cm^{-1} also showed a minor shift, suggesting modified lipid packing in the SLNs.

Overall, the FTIR spectra confirmed the successful encapsulation of dasatinib into the SLNs. The preservation of major peaks alongside minor shifts and intensity changes suggest that dasatinib is physically entrapped within the lipid matrix rather than undergoing covalent modification. These spectral modifications point to weak intermolecular interactions—such as hydrogen bonding and Van der Waals forces—between dasatinib and stearic acid, which support stable encapsulation within the SLNs.

3.2.2. Differential Scanning Calorimetry (DSC) Analysis

DSC analysis was employed to evaluate the thermal behavior and physical state of dasatinib, stearic acid, and the dasatinib-loaded solid lipid nanoparticles (SLNs). The thermograms (Figure 6) of pure dasatinib exhibited a sharp endothermic peak at 284.54 °C, corresponding to its characteristic melting point, which is indicative of its highly crystalline nature. Stearic acid showed a distinct melting peak at 69.31 °C, consistent with literature values, reflecting its crystalline lipid matrix.

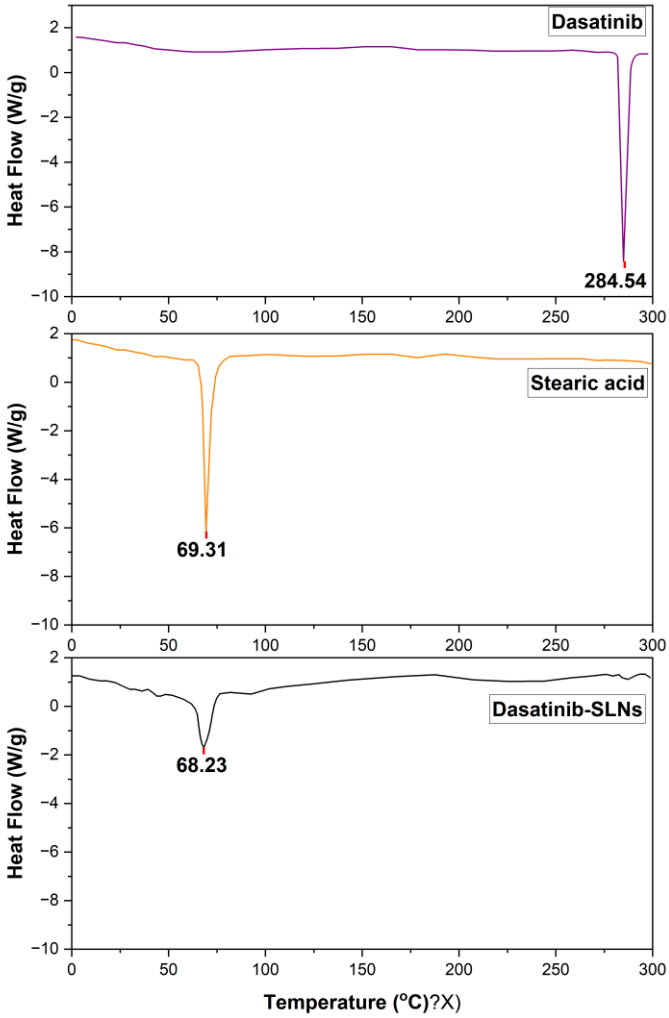

Figure 6: DSC thermograms of Dasatinib, stearic acid and Dsastinib-SLNs

In contrast, the DSC thermogram of dasatinib-stearic acid SLNs demonstrated a single broadened endothermic peak at 68.23 °C, while the sharp melting peak of dasatinib at 284.54 °C was absent. The disappearance of the drug's melting peak suggests that dasatinib is no longer in its crystalline form but is instead molecularly dispersed or encapsulated in an amorphous state within the lipid matrix. Furthermore, the slight depression and broadening of the stearic acid melting peak in the SLNs, compared to its pure form, indicates a reduction in lipid crystallinity due to the presence of the drug and possible interactions between the drug and lipid components.

These observations confirm the successful incorporation of dasatinib into the lipid matrix, leading to a partial amorphization and disruption of the ordered structure of stearic acid. Such modifications are desirable in lipid-based nanoparticulate systems, as they are known to enhance drug solubility, dispersion, and release profiles. Therefore, the DSC results provide strong evidence of the formation of dasatinib-

loaded SLNs with improved physicochemical characteristics suitable for oral drug delivery.

3.2.3. SEM Analysis

The SEM image (Figure 7) of dasatinib-loaded SLNs shows uniformly distributed, spherical particles with smooth surfaces, indicating successful nanoparticle formation and good physical stability. The absence of drug crystals suggests effective encapsulation of dasatinib within the lipid matrix. Particle sizes appear in the micrometre range, favouring improved absorption and bioavailability. The morphology reflects efficient emulsification and solidification, confirming the suitability of the formulation process for enhanced drug delivery.

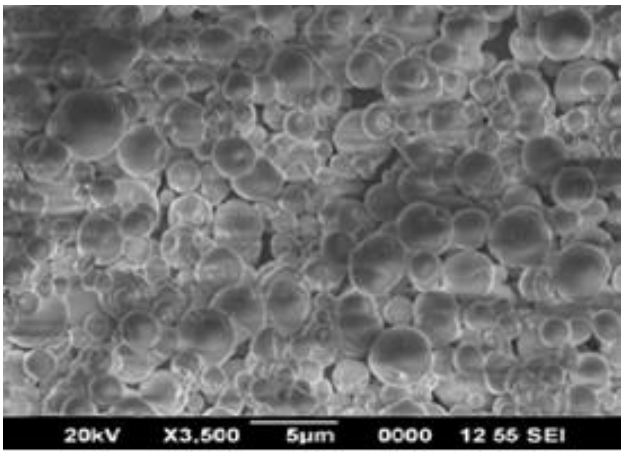

Figure 7: SEM image of optimized Dasatinib-SLNs

3.2.4. *In vitro* Drug release

The dissolution profile presented in Table 3 highlights the comparative in vitro drug release behaviour of the optimized Dasatinib-loaded solid lipid nanoparticles (SLNs) and the marketed Dasatinib tablet in 0.1N HCl medium over a 24-hour period. The marketed Dasatinib tablet exhibited a rapid and nearly complete drug release within the initial few hours, reaching 76.67 ± 1.06% within 30 minutes and 81.40 ± 0.95% at 2 hours. This rapid release profile suggests a burst release from the conventional formulation, which may lead to higher peak plasma concentrations and potential fluctuations in systemic drug levels. In contrast, the Dasatinib-SLNs showed a markedly sustained release pattern. At the same 2-hour time point, the SLNs released only 16.38 ± 1.05% of the drug. The release from the SLNs progressed gradually, reaching 53.97 ± 1.48% at 8 hours and 75.55 ± 1.35% at 12 hours, with a near-complete release of 95.39 ± 1.78% achieved only at 24 hours. This indicates a controlled and prolonged release of Dasatinib from the SLN matrix.

Table 3: Summary of dissolution data of Dasatinib-SLNs and pure Dasatinib

Time Interval (Hours)	% Cumulative drug released from optimized Dasatinib-SLNs (0.1N)	% Cumulative drug released from Dasatinib (Marketed tablet) (0.1N HCl medium)
0.5	5.21 ± 0.73	76.67 ± 1.06
1	9.88 ± 0.93	78.54 ± 1.04
2	16.38 ± 1.05	81.40 ± 0.95
4	27.99 ± 1.30	84.01 ± 0.54
6	41.04 ± 0.96	86.16 ± 1.01
8	53.97 ± 1.48	88.24 ± 0.47
10	60.67 ± 1.40	91.29 ± 0.85
12	75.55 ± 1.35	93.72 ± 0.61
18	92.24 ± 1.78	95.66 ± 0.31
24	95.39 ± 1.78	96.58 ± 0.38

The sustained release behaviour of the SLNs can be attributed to the encapsulation of Dasatinib within the solid lipid matrix, which creates a diffusion barrier, and the stabilizing effect of surfactants that modulate release kinetics. This slower release is beneficial for maintaining consistent plasma drug levels over time, potentially reducing dosing frequency and improving patient adherence in therapeutic applications. Overall, the SLN formulation demonstrated a desirable controlled-release profile in contrast to the immediate-release behaviour of the marketed tablet. This extended-release characteristic of Dasatinib-SLNs underscores their potential for improved oral delivery of poorly water-soluble anticancer agents like Dasatinib, offering enhanced bioavailability and reduced dosing-related side effects.

3.2.5. Release Kinetics Analysis of Dasatinib-Loaded SLNs

The in vitro dissolution profile of optimized Dasatinib-loaded solid lipid nanoparticles (SLNs) was systematically evaluated using five pharmacokinetic models to elucidate the underlying release mechanism. Model selection was based on rigorous statistical criteria, prioritizing the highest correlation coefficient (R^2) and lowest Akaike Information Criterion (AIC). Among the tested models, the Korsmeyer-Peppas equation demonstrated superior fit (R^2 = 0.995, AIC = 9.2), with parameters kk=14.25kk =14.25 and n=0.56n=0.56.

The release exponent (n=0.56n=0.56) indicated non-Fickian (anomalous) diffusion, signifying a combined mechanism of drug diffusion and lipid matrix erosion. This dual-phase process was further reflected in the dissolution profile: an initial burst release (~16% at 2 h) attributed to surface-adsorbed drug, followed by sustained release (2–18 h) governed by diffusion through the lipid core, and near-complete release (95% at 24 h) driven by matrix degradation.

The Higuchi model (R^2 = 0.988) and first-order kinetics (R^2 = 0.972) provided partial fits but failed to capture the full release trajectory, while zero-order and Hixson-Crowell models were inadequate (R^2 < 0.965). The dominance of anomalous transport aligns with the expected

behaviour of SLNs, where drug release is modulated by both lipid crystallinity and environmental erosion.

Clinically, this controlled release profile offers significant advantages over immediate release dasatinib, including prolonged therapeutic action and reduced dosing frequency, which may enhance patient compliance and bioavailability.

3.2.6. *In-vivo* Pharmacokinetics

The pharmacokinetic parameters of the optimized Dasatinib-loaded solid lipid nanoparticles (SLNs) were compared with those of Dasatinib marketed formulation following oral dose of 10 mg. The summary of major pharmacokinetic parameter was disclosed in Table 4 and figure 8. A marked improvement in the pharmacokinetic profile was observed for Dasatinib-SLNs, indicating enhanced oral bioavailability and sustained drug release.

The time to reach maximum plasma concentration (T_{max}) for Dasatinib-SLNs was significantly delayed to 8 hours compared to 2 hours for pure Dasatinib. This prolonged T_{max} reflects the sustained release nature of the SLN formulation, which enables gradual drug absorption over an extended period.

Although the maximum plasma concentration (Cmax) of Dasatinib-SLNs (1194.92 ng/mL) was slightly lower than that of pure Dasatinib (1423.85 ng/mL), the overall exposure, as indicated by AUC_{last} (12424.05 ng·h/mL) and AUC_∞ (12643.32 ng·h/mL), was significantly higher than for pure Dasatinib (7765.68 ng·h/mL and 7849.62 ng·h/mL, respectively). This 1.6-fold increase in AUC underscores the improved systemic availability of the drug from the SLN formulation, likely due to enhanced solubilization, prolonged gastrointestinal residence, and lymphatic absorption.

Table 4: Summary of pharmacokinetic parameters of Dasatinib-SLNs and Dasatinib

Parameter	Units	Dasatinib-SLNs	Dasatinib
Dose	mg	10	10
Time to Maximum Concentration (T_{max})	h	8*	2
Maximum Plasma Concentration (C_{max})	ng/mL	1194.92**	1423.85
Terminal Half-Life (t½)	h	9.5**	3.4
Area Under the Curve, Last (AUC_{last})	ng·h/mL	12424.05*	7765.68*
Area Under the Curve, Infinity Observed (AUC_{INF_obs})	ng·h/mL	12643.32	7849.62
Percentage of AUC Extrapolated Observed ($AUC\_\%_{Extrap\_obs}$)	%	11.85	1.06
Apparent Volume of Distribution/F (Vz/F_obs)	L/kg	0.00897	0.00306
Apparent Clearance/F (Cl/F_obs)	L/h/kg	0.000803	0.00124
Mean Residence Time, Infinity Observed (MRTINF_obs)	h	10.92	5.37

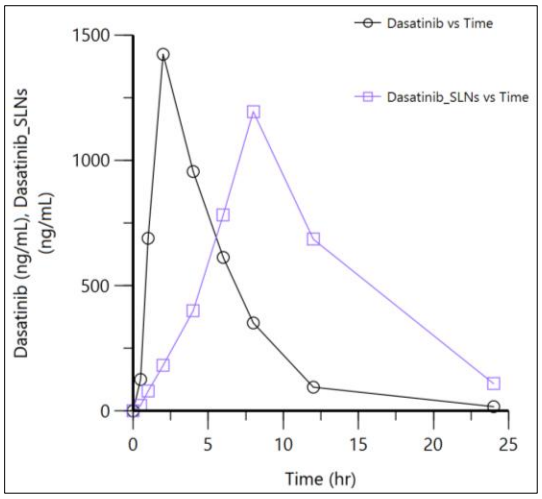

Figure 8: Plasma Concentration–Time Profile of Dasatinib and Dasatinib-Loaded SLNs Following Oral Administration in Rats

The terminal half-life (t½) of Dasatinib-SLNs was extended to 9.5 hours, compared to 3.4 hours for pure Dasatinib, confirming the sustained release behaviour of the SLN system. Correspondingly, the mean residence time ($MRT_{(\infty)}$) for Dasatinib-SLNs (10.92 h) was approximately twice that of pure Dasatinib (5.37 h), indicating prolonged systemic circulation.

In terms of disposition kinetics, Dasatinib-SLNs exhibited a lower apparent clearance (Cl/F_obs = 0.000803 L/h/kg) and a larger apparent volume of distribution (Vz/F_obs = 0.00897 L/kg) compared to the pure drug. These findings suggest reduced elimination and better tissue distribution of Dasatinib when delivered via SLNs.

While the percentage of AUC extrapolated (AUC_%Extrap_obs) was slightly higher for the SLNs (11.85%) than for the pure drug (1.06%), it remained within acceptable limits, ensuring reliable estimation of total drug exposure.

4. CONCLUSION

The systematic optimization of Dasatinib-SLNs using a Box-Behnken design successfully yielded nanoparticles with optimal physicochemical properties (size < 210 nm, high EE > 85%, and stability-inducing zeta potential). The formulation's sustained release profile, governed by non-Fickian diffusion, addresses the limitations of conventional Dasatinib tablets, which exhibit rapid release and suboptimal pharmacokinetics. In vivo studies validated the SLNs' ability to enhance bioavailability (AUC: 1.6-fold) and prolong drug circulation (t½: 2.8-fold), likely due to lymphatic uptake and reduced first-pass metabolism.

Acknowledgement

The authors are grateful to the Department of Pharmaceutics, Motherhood University, Roorkee, Uttarakhand, India, for providing the necessary facilities for the successful completion of this work.

Author Contribution

All authors contributed equally with current work.

Conflict of interest

Authors disclose no conflict of interest with current work.

REFERENCES

1. Santos, F. P., & Cortes, J. (2012). Dasatinib for the treatment of Philadelphia chromosome-positive leukemias. Expert opinion on pharmacotherapy, 13(16), 2381–2395. https://doi.org/10.1517/14656566.2012.725722
2. Lindauer, M., & Hochhaus, A. (2014). Dasatinib. Recent results in cancer research. Fortschritte der Krebsforschung. Progres dans les recherches sur le cancer, 201, 27–65. https://doi.org/10.1007/978-3-642-54490-3_2
3. Araujo, J., & Logothetis, C. (2010). Dasatinib: a potent SRC inhibitor in clinical development for the treatment of solid tumors. Cancer treatment reviews, 36(6), 492–500. https://doi.org/10.1016/j.ctrv.2010.02.015
4. Begum, M. N., Khan, M. A., Ara, T., Biswas, A. R., Akter, M., Islam, M. M., Nazneen, H., & Farhad, M. N. (2024). Response of dasatinib in different phase of chronic myeloid leukaemia patients. *International Journal of Research in Medical Sciences*, *13*(1), 33–38. https://doi.org/10.18203/2320-6012.ijrms20244091
5. Kennedy, J. A., & Hobbs, G. (2018). Tyrosine Kinase Inhibitors in the Treatment of Chronic-Phase CML: Strategies for Frontline Decision-making. Current hematologic malignancy reports, 13(3), 202–211. https://doi.org/10.1007/s11899-018-0449-7
6. Samineni, R., Chimakurthy, J., & Konidala, S. (2022). Emerging Role of Biopharmaceutical Classification and Biopharmaceutical Drug Disposition System in Dosage form Development: A Systematic Review. Turkish journal of pharmaceutical sciences, 19(6), 706–713. https://doi.org/10.4274/tjps.galenos.2021.73554
7. Abdul Azeeze, M. S. T., Kandasamy, S., Palanisamy, P., Palanichamy, P., & Nainar, M. S. (2023). Cocrystallization of Dasatinib with different acids improves the solubility and physicochemical properties: A combined experimental and theoretical studies. Chemical Physics Impact, 7, 100247. https://doi.org/10.1016/j.chphi.2023.100247
8. O Brien, Z., & Moghaddam, M. F. (2017). A Systematic Analysis of Physicochemical and ADME Properties of All Small Molecule Kinase Inhibitors Approved by US FDA from January 2001 to October 2015. Current medicinal chemistry, 24(29), 3159–3184. https://doi.org/10.2174/0929867324666170523124441
9. Roskoski R., Jr (2021). Properties of FDA-approved small molecule protein kinase inhibitors: A 2021 update. Pharmacological research, 165, 105463. https://doi.org/10.1016/j.phrs.2021.105463
10. Kovar, C., Loer, H. L. H., Rüdesheim, S., Fuhr, L. M., Marok, F. Z., Selzer, D., Schwab, M., & Lehr, T. (2024). A physiologically-based pharmacokinetic precision dosing approach to manage dasatinib drug-drug interactions. CPT: pharmacometrics & systems pharmacology, 13(7), 1144–1159. https://doi.org/10.1002/psp4.13146
11. Levêque, D., Becker, G., Bilger, K., & et al. (2020). Clinical pharmacokinetics and pharmacodynamics of dasatinib. Clinical Pharmacokinetics, 59, 849–856. https://doi.org/10.1007/s40262-020-00872-4
12. Ghasemiyeh, P., & Mohammadi-Samani, S. (2018). Solid lipid nanoparticles and nanostructured lipid carriers as novel drug delivery systems: applications, advantages and disadvantages. Research in pharmaceutical sciences, 13(4), 288–303. https://doi.org/10.4103/1735-5362.235156
13. Akanda, M., Mithu, M. S. H., & Douroumis, D. (2023). Solid lipid nanoparticles: An effective lipid-based technology for cancer treatment. Journal of Drug Delivery Science and Technology, 86, 104709. https://doi.org/10.1016/j.jddst.2023.104709
14. Arabestani, M. R., Bigham, A., Kamarehei, F., Dini, M., Gorjikhah, F., Shariati, A., & Hosseini, S. M. (2024). Solid lipid nanoparticles and their

application in the treatment of bacterial infectious diseases. Biomedicine & Pharmacotherapy, 174, 116433. https://doi.org/10.1016/j.biopha.2024.116433

15. Mishra, V., Bansal, K. K., Verma, A., Yadav, N., Thakur, S., Sudhakar, K., & Rosenholm, J. M. (2018). Solid Lipid Nanoparticles: Emerging Colloidal Nano Drug Delivery Systems. Pharmaceutics, 10(4), 191. https://doi.org/10.3390/pharmaceutics10040191
16. Mukherjee, S., Ray, S., & Thakur, R. S. (2009). Solid lipid nanoparticles: a modern formulation approach in drug delivery system. Indian journal of pharmaceutical sciences, 71(4), 349–358. https://doi.org/10.4103/0250-474X.57282
17. Rostami, E., Kashanian, S., Azandaryani, A. H., Faramarzi, H., Dolatabadi, J. E., & Omidfar, K. (2014). Drug targeting using solid lipid nanoparticles. Chemistry and physics of lipids, 181, 56–61. https://doi.org/10.1016/j.chemphyslip.2014.03.006
18. Vitorino, C., Carvalho, F. A., Almeida, A. J., Sousa, J. J., & Pais, A. A. (2011). The size of solid lipid nanoparticles: an interpretation from experimental design. *Colloids and surfaces B: biointerfaces*, *84*(1), 117-130.
19. Onugwu, A. L., Attama, A. A., Nnamani, P. O., Onugwu, S. O., Onuigbo, E. B., & Khutoryanskiy, V. V. (2022). Development and optimization of solid lipid nanoparticles coated with chitosan and poly(2-ethyl-2-oxazoline) for ocular drug delivery of ciprofloxacin. Journal of Drug Delivery Science and Technology, 74, 103527. https://doi.org/10.1016/j.jddst.2022.103527
20. Elbrink, K., Van Hees, S., Holm, R., & Kiekens, F. (2023). Optimization of the different phases of the freeze-drying process of solid lipid nanoparticles using experimental designs. International Journal of Pharmaceutics, 635, 122717. https://doi.org/10.1016/j.ijpharm.2023.122717